

Independently controlling permittivity and diamagnetism in broadband, low-loss, isotropic metamaterials at microwave frequencies

L. Parke, I. R. Hooper, E. Edwards, N. Cole, I. J. Youngs, A. P. Hibbins, and J. R. Sambles

Citation: [Applied Physics Letters](#) **106**, 101908 (2015); doi: 10.1063/1.4915097

View online: <http://dx.doi.org/10.1063/1.4915097>

View Table of Contents: <http://scitation.aip.org/content/aip/journal/apl/106/10?ver=pdfcov>

Published by the [AIP Publishing](#)

Articles you may be interested in

[Low-loss negative index metamaterials for X, Ku, and K microwave bands](#)

[AIP Advances](#) **5**, 047119 (2015); 10.1063/1.4918283

[Metamaterial waveguides with highly controllable negative-permittivity bands](#)

[Appl. Phys. Lett.](#) **105**, 241111 (2014); 10.1063/1.4904477

[Triple band polarization-independent ultra-thin metamaterial absorber using electric field-driven LC resonator](#)

[J. Appl. Phys.](#) **115**, 064508 (2014); 10.1063/1.4865273

[Low-loss NiCuZn ferrite with matching permeability and permittivity by two-step sintering process](#)

[J. Appl. Phys.](#) **113**, 17B301 (2013); 10.1063/1.4793508

[Broadband and low loss high refractive index metamaterials in the microwave regime](#)

[Appl. Phys. Lett.](#) **102**, 091108 (2013); 10.1063/1.4794088

Frustrated by old technology? Is your AFM dead and can't be repaired? Sick of bad customer support?



It is time to upgrade your AFM
Minimum \$20,000 trade-in discount for purchases before August 31st

Asylum Research is today's technology leader in AFM

dropmyoldAFM@oxinst.com

OXFORD INSTRUMENTS
The Business of Science®

Independently controlling permittivity and diamagnetism in broadband, low-loss, isotropic metamaterials at microwave frequencies

L. Parke,¹ I. R. Hooper,¹ E. Edwards,² N. Cole,¹ I. J. Youngs,³ A. P. Hibbins,¹ and J. R. Sambles¹

¹*Electromagnetic and Acoustic Materials Group, Department of Physics and Astronomy, University of Exeter, Stocker Road, Exeter, EX4 4QL, United Kingdom*

²*Department of Materials, University of Oxford, Parks Road, Oxford, OX1 3PH, United Kingdom*

³*Defence Science and Technology Laboratory, Salisbury, SP4 0JQ, United Kingdom*

(Received 1 December 2014; accepted 5 March 2015; published online 12 March 2015)

A metamaterial based on the design of Shin *et al.* [Phys. Rev. Lett. **102**, 093903 (2009)] that allows independent control of its permeability and permittivity has been fabricated and experimentally characterised. It is comprised of an array of metallic cubic-shaped elements with faces that are connected only through six orthogonal spokes emanating from the centre. The permeability is tailored through appropriate patterning of the faces, thereby controlling the propagation of eddy currents around the cubic elements while permittivity may be controlled by the thickness and dielectric constant of the inter-cube spacers. © 2015 AIP Publishing LLC. [<http://dx.doi.org/10.1063/1.4915097>]

Metamaterials are artificial structures, where the electromagnetic properties are dictated by geometry in addition to the composition of the material.^{1–3} Such materials are comprised of arrays of sub-wavelength elements arranged such that the interaction between individual elements with an incident electromagnetic field provides a collective effective-medium response yielding bespoke values of complex relative permeability $\mu_r = \mu'_r + i\mu''_r$ and complex relative permittivity $\epsilon_r = \epsilon'_r + i\epsilon''_r$. This has led to the creation of metamaterials with exotic properties such as negative refractive index,^{1,4} very high refractive index,⁵ and impedance-matched high refractive indices.⁶ Methods for realising such properties typically rely on electromagnetic resonances, therefore suffering from a narrow operating frequency range and significant magnetic and dielectric losses.¹ By comparison, if such properties could be achieved in a metamaterial in a non-resonant manner, the response could be broadband⁵ with low-losses. This gives electromagnetic properties desirable for the creation of graded index devices.⁷

Consider first how one may achieve a high refractive index metamaterial comprised of a cubic array of sub-wavelength metallic cubes such as those illustrated in Figure 1. The real part of the effective permittivity is relatively simple to control. By exploiting the capacitive coupling between adjacent cubes (e.g., by varying the gap between them), values of $\epsilon'_r \gg 1$ can be achieved.⁸ However, since the cubic elements are metallic, they also exhibit a diamagnetic response ($\mu'_r \sim 0$) due to the propagation of eddy currents on the surface of the cube, limiting the achievable refractive index ($n = \text{Re}\sqrt{\mu_r \epsilon_r}$). Thus, in order to generate high refractive index metamaterials formed from cubic metallic elements, one needs to weaken the diamagnetic response (increase μ'_r towards 1).

Tailoring the diamagnetic response of non-resonant metamaterials has previously been investigated by Lapine *et al.*⁹ who aimed to achieve a *near zero* value of μ'_r : a theoretical μ'_r of 0.05 was obtained using a close packed hexagonal lattice of closed metallic loops. Further developments by

Belov *et al.*¹⁰ reported slightly higher values of μ'_r but importantly produced an isotropic metamaterial consisting of an array of metallic cubes, resulting in μ'_r values of 0.15. In contrast to the above work, Shin *et al.*¹¹ aim to produce high refractive index metamaterials and hence a *near unity* value of μ'_r . Shin *et al.* developed the design of Belov *et al.* further and showed numerically that it was possible to significantly weaken the diamagnetic response of cubic metamaterial structures through appropriate structuring (increasing μ'_r towards 1, allowing for the refractive index to be greatly enhanced). The approach of Shin *et al.* consisted of a two-stage modification to a simple cubic array of solid metallic cubes that, in its simplest form, is an array of cubes (Figure 1(a)), with $a = 10$ mm possessed an enhanced ϵ'_r of approximately 20 but a μ'_r of approximately 0.1 from 10 to 500 MHz. In the first stage, they replaced the solid cubes with hollow cubes, each having separated faces that were only electrically connected through the centre of the cube by six conducting spokes (see Figure 1(b)). This results in a weakened diamagnetic response: μ'_r being increased from 0.1 to 0.57 for the progression from the solid cube array to the array of hollow cubes with separated faces designed by Shin *et al.* The significant weakening is due to the confining of the currents to the edge of two plates perpendicular to the applied magnetic field and to the faces of the four plates parallel to the applied magnetic field. This has been experimentally verified by Campbell *et al.* in 2013.¹² In the second stage, Shin *et al.* subdivided each face (see Figure 1(c)) to limit the area enclosed by surface currents, thereby decreasing the diamagnetic response and increasing μ'_r to a value of 0.97 whilst maintaining the large increase in ϵ_r . In this study, we verify that subdividing the plates does indeed weaken the diamagnetic response as proposed by Shin *et al.* and demonstrate thereby a high refractive index metamaterial for the microwave regime. We study three different metamaterial samples, initially via numerical modelling, before fabricating, and characterising their electromagnetic response over the frequency range from 10 MHz to 500 MHz. Schematics

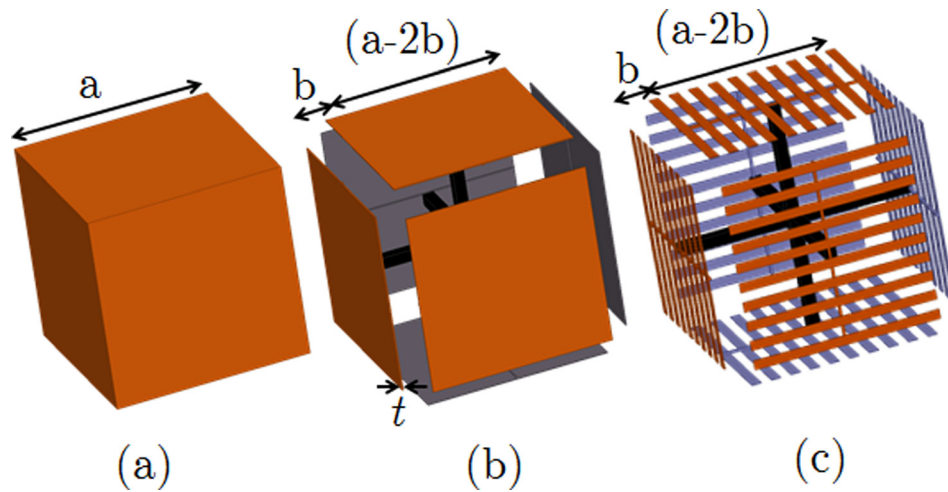


FIG. 1. (a) A schematic of a solid copper cube metamaterial element with face areas of a^2 . (b) A hollow copper cube metamaterial element with face areas of $(a - 2b)^2$. The faces of the cube are disconnected along the edges and joined together by orthogonal metal spokes that connect at the centre of the cube. The variable t denotes the plate thickness in both (b) and (c). (c) A progression from (b) where each face of the cube has now been subdivided to produce a “comb” like structured face. Once again, all six faces are electrically connected through the centre of the cube (Note that only 10 of the 20 rods on each face have been drawn for clarity).

of the three individual elements of the three metamaterials studied are shown in Figure 1.

Consider a plane wave normally incident upon the surface of a semi-infinite 3D cubic array formed from each element. For the array formed of solid metallic cubes (Figure 1(a)), the propagation of eddy currents around the whole cube produces a strong diamagnetic response. The hollow plated cube (Figure 1(b)) reduces the area enclosed by the induced currents by confining them to the individual faces (four faces parallel to the incident magnetic field and two faces perpendicular to the incident magnetic field). The two plates perpendicular to the applied magnetic field provide the largest contribution to the diamagnetic response, since the induced current extends around the entire area of each plate with an area of $(a - 2b)^2 = 64 \text{ mm}^2$. The plate thickness also alters the diamagnetic properties of the cube arrays. In the case where the plates are perpendicular to the applied magnetic field, increasing the plate thickness leads to increase in the integral of the current density, which strengthens the diamagnetic response. By contrast, the four plates parallel to the applied magnetic field produce a far weaker diamagnetic response, since the current loops only extends around the narrow edge of the plates, each presenting an area of $(a - 2b)t = 0.56 \text{ mm}^2$. Now consider the permittivity: since the effective ϵ'_r of the metamaterial is determined by the capacitive coupling between the plates of adjacent elements, it is dependent upon the spacing between them in the direction perpendicular to the incident electric field, the face size, and the permittivity of the spacer material between them. The reduction in the area of the faces in going from solid cubes to plates ($100 \text{ mm}^2 - 64 \text{ mm}^2$) reduces the capacitance and hence the permittivity, but the second refinement, from solid plates to subdivided plates, does not result in significant further reduction.

The solid cube array was fabricated by spacing $10 \times 10 \times 10 \text{ mm}$ solid copper cubes (shown in Fig. 1(a)) with bare FR4 laminate (permittivity of $4.4 + 0.02i$) of thickness 0.8 mm , which provides a 1.6 mm gap between adjacent

cubes. To fabricate the array of cubes with plated and structured faces, copper-clad FR4 circuit board was etched so as to produce an array of $8 \times 8 \text{ mm}$ square patches (for the plated faces) and $8 \times 8 \text{ mm}$ arrays of twenty connected 0.3 mm wide rods (for the structured faces) of thickness $35 \mu\text{m}$. The boards were assembled to form two $6 \times 5 \times 1$ arrays. Opposite cube faces were electrically connected through the centre of the cube by soldering wire onto each face to join at the centre, as illustrated in Figure 2.

Two samples of each design were positioned above and below the central conducting line in a calibrated stripline of a similar design to that of Barry,¹³ but designed such that the stripline was impedance-matched throughout the frequency range of interest ($10 \text{ MHz} - 4 \text{ GHz}$) with no sample present (Figure 3). The stripline was connected to a vector network analyser (VNA) and the S-parameters (the complex reflection and transmission co-efficients) were recorded. Since

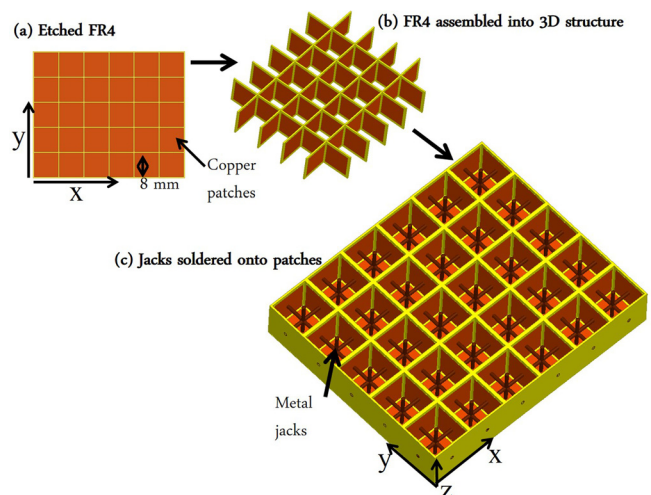


FIG. 2. Fabrication of structured cubic metamaterials. (a) Single sided FR4 circuit board with $8 \times 8 \text{ mm}$ copper squares or 0.3 mm rods etched onto the metallic side, (b) etched circuit board cut and assembled into a 3D structure, and (c) central rods are soldered to opposing cube faces, and the top and bottom sheets are attached.

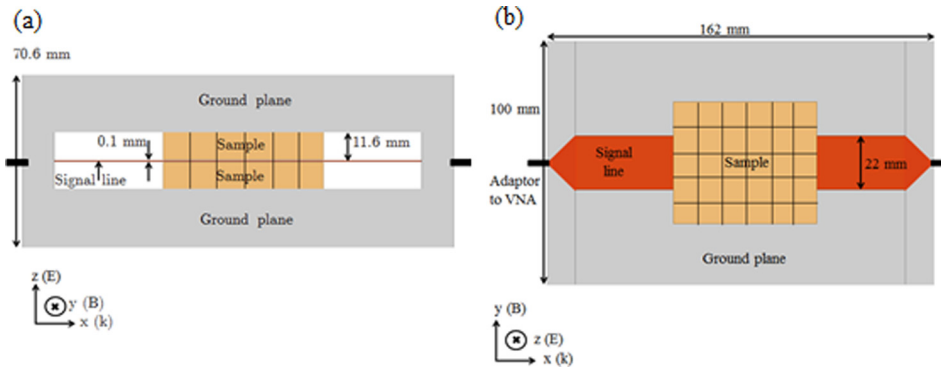


FIG. 3. Schematic of the stripline set up containing the metamaterial sample: (a) side-on view and (b) top-down view.

each cube array was much wider (width = 56.4 mm) than the signal line (width = 22 mm), and since the presence of the ground planes above and below the cube arrays mimic an infinitely repeating array of cubic elements in the electric field direction (z -direction), the measured S-parameters were equivalent to those that one would obtain from a sample of infinite extent in the y - and z -directions.

The effective μ_r and ϵ_r of the metamaterials was determined in the frequency range of 10–500 MHz, using a fitting algorithm (implemented using the *fmincon* function in Matlab¹⁴), which simultaneously fits the real and imaginary parts of the S-parameters to the well-known three layer Fresnel equations for normal incidence reflection and transmission through a parallel sided slab

$$r_{13} = r_{12} + \frac{t_{12}t_{21}r_{23}e^{2i\alpha}}{1 - r_{21}r_{23}e^{2i\alpha}}, \quad (1)$$

$$t_{13} = \frac{t_{12}t_{23}e^{2i\alpha}}{1 - r_{21}r_{23}e^{2i\alpha}}, \quad (2)$$

using the sum of squares difference between the measured and calculated values as the objective function. Here, t_{13} , t_{12} , t_{21} , and t_{23} are the complex transmission amplitude

coefficients; r_{13} , r_{12} , r_{21} , and r_{23} are the complex reflection amplitude coefficients; and $e^{2i\alpha}$ is the phase factor. Since this method fits to all data points simultaneously, it can only be used when the material properties are non-dispersive and, as will become clear below, this limits the frequency range of characterisation for the measured samples to between 10 and 500 MHz. The same fitting routine has been successfully utilised previously by Campbell *et al.*¹² when investigating plated cube arrays.

Before implementing the fitting routine method, one first needs to determine the frequency range over which the material properties are non-dispersive. This is easy to deduce for any of the three samples by examining a plot of the reflected and transmitted intensities calculated from the S-parameters as a function of frequency. Such plots are shown in Figure 4, along with finite element method modelling of the systems calculated using Ansys HFSS.¹⁵ Experimental data (Figure 4(a)) show a minimum at zero frequency followed by 4 distinct reflection minima. These correspond to the excitation of standing wave eigenmodes within the first Brillouin zone of the six unit cell repeat structure. It is apparent that the eigenmodes for each of the three different metamaterials are not equally spaced in frequency, with the peaks becoming

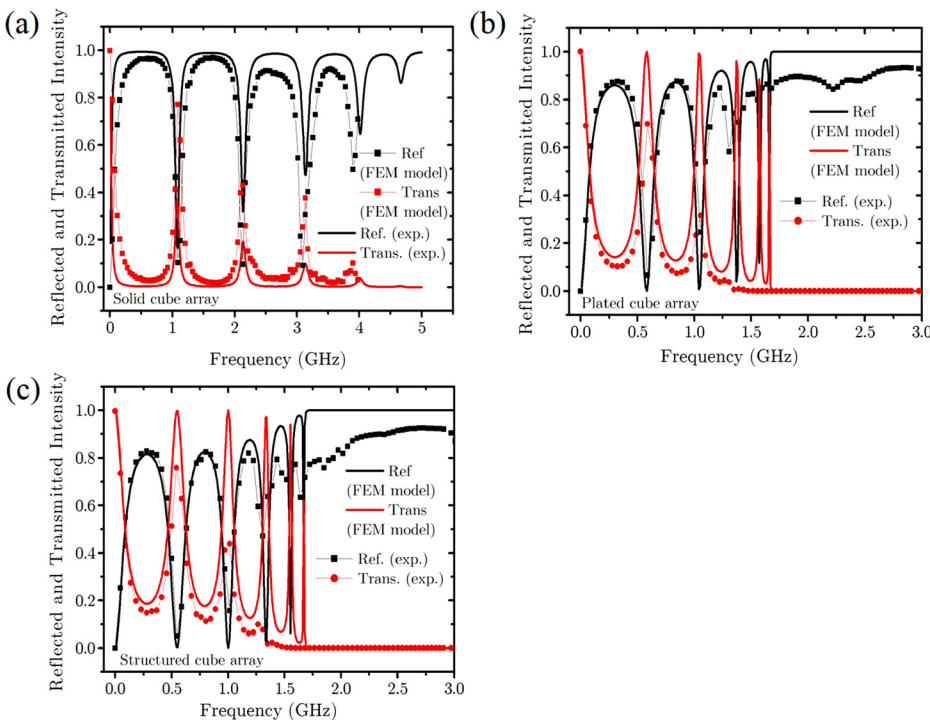


FIG. 4. Reflected and transmitted intensity as a function of frequency for (a) the solid cube array, (b) the plated cube array, and (c) the structured cube array. Each plot shows both experimental results (points) and FEM numerical modelling results (solid lines).

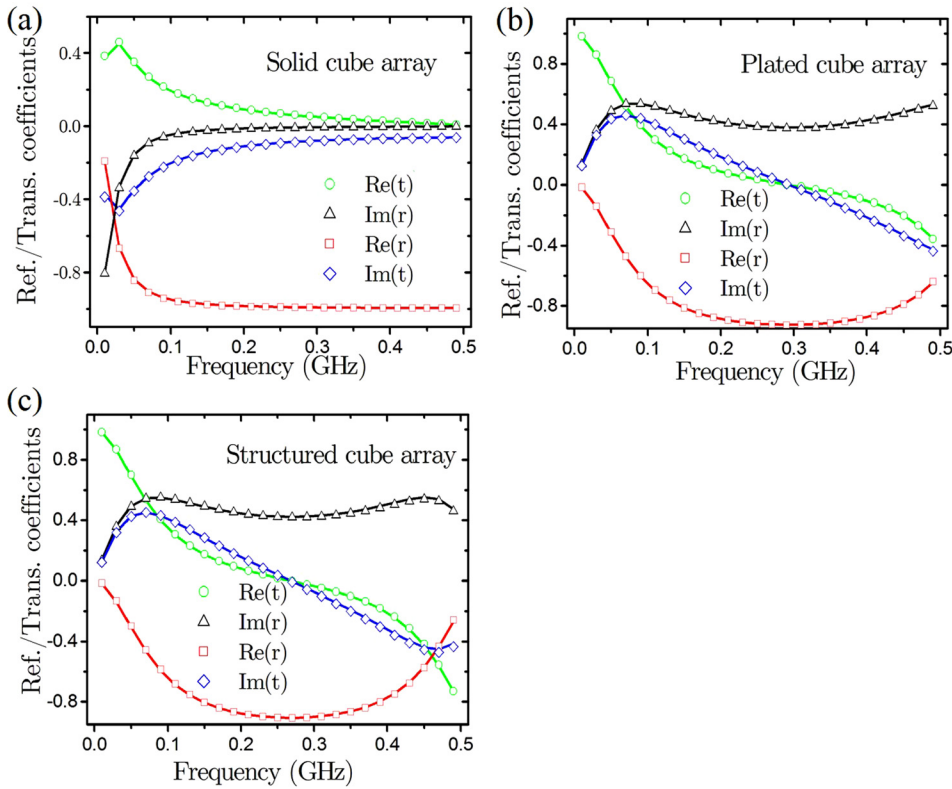


FIG. 5. Comparison between experiment (lines) and Fresnel fitting algorithm fits (open circles) for the reflected and transmitted amplitude coefficients as a function of frequency for: (a) the solid cube array, (b) the plated cube array, and (c) the structured cube array.

closer together with increasing frequency as the Brillouin zone boundary in reciprocal space is approached. This non-uniform spacing clearly illustrates dispersion. Notice how, compared to the simple cube array the plated and structured cube arrays have transmission peaks that are compressed to lower frequencies due to the higher effective refractive index. One also observes the photonic band gap at frequencies above the 5th resonance within which no power is transmitted through the metamaterial samples. The non-unity sum of the reflection and transmission is indicative of losses in the metamaterial and is associated with the loss tangent inherently present in the FR4 circuit board. One can simply estimate the low-frequency effective refractive index of the metamaterials through consideration of the position in frequency of the first peak, found at 1.08 GHz for the solid cubes, 0.60 GHz for the plated cubes, and 0.54 GHz for the structured plated cubes, corresponding to refractive indices of 2.0, 3.7, and 4.1, respectively.

From analysis of the mode positions in Figure 4, one can identify a low frequency band over which the effective material properties are non-dispersive between 10 MHz and 500 MHz. Thus, one can utilise the fitting routine method for extracting the effective μ_r and ϵ_r over this frequency band. The results of this process are shown in Figure 5, where the real and imaginary parts of the measured and fitted reflection and transmission amplitude coefficients are plotted as a function of frequency, from these fits, values for μ_r and ϵ_r are deduced, as well as the refractive index, n , for each of the three types of cube array. These values are given in Table I and, not surprisingly, the values of n are almost the same as that naively estimated above.

Table I shows the extracted electromagnetic parameters from each of the 3 different types of metamaterial sample, with each having been independently measured three times

to estimate the experimental uncertainty. The increase in permeability in the progression from solid cube arrays to arrays of structured cubes demonstrates that the structuring greatly suppresses eddy currents as expected. In addition to our previous discussion regarding the origin of the diamagnetic response arising from induced currents on the faces of the cubic structures, we have used FEM modelling to analyse the effect on the circulating currents, and hence the diamagnetism, of the thickness of the plates. For the 2 pairs of faces parallel to the applied magnetic field, the diamagnetic response is weak with the current loops having a small area which leads to an approximately linear relationship between μ'_r and these plate thicknesses, with μ'_r decreasing as the plates thicken. For the 2 pairs of faces perpendicular to the applied magnetic field, the plate thickness does not impact the area of the current loop but instead alters the integrated magnitude of the current, which increases with increasing plate thickness, leading to an inverse relationship between μ'_r and the plate thicknesses. It is then apparent that using very thin metal, say, copper less than 20 μm thick, is beneficial for producing permeabilities of near unity and thus higher refractive indices. (Note that once the metal thickness is less than the skin-depth thick, this simplistic view fails.)

TABLE I. The relative real permeability, permittivity, and refractive index for the solid, plated, and structured cube arrays in the frequency band from 10 to 500 MHz as extracted from the Fresnel fitting algorithm.

	ϵ'_r	μ'_r	n
Solid cube array	26 ± 1	0.13 ± 0.02	1.8 ± 0.2
Plated cube array	19 ± 1	0.72 ± 0.02	3.7 ± 0.2
Structured cube array	18 ± 2	0.92 ± 0.03	4.1 ± 0.1

ϵ'_r only falls from 19 to 18 when progressing from the plated cube array to the structured cube array. Provided the slats on the structured cubes are close enough together, the slats screen out the incident electric field and hence produce the same dielectric response as a solid face (acting essentially like a wire grid polariser). To further increase ϵ'_r , a material of higher ϵ'_r than FR4, or having a reduced thickness, should be placed between the cubes. Such modifications of the existing structures will provide a route to exceptionally high and, potentially, spatially variable refractive index metamaterials with independent control of the electromagnetic parameters within the constraints that $\epsilon'_r > 1$ and $0 < \mu'_r < 1$.

In conclusion, a high refractive index broadband (10–500 MHz) metamaterial has been designed and fabricated that allows independent control of both its effective permeability and effective permittivity. We have demonstrated that, by appropriately structuring arrays of metallic cubes, it is possible to maintain a high effective permittivity whilst weakening the usual diamagnetic response, increasing the permeability from a value of 0.13 ± 0.02 (strongly diamagnetic) for solid metallic cubes to 0.90 ± 0.05 for our structured cubes. The permittivity undergoes a corresponding decrease from 26 ± 2 to 18 ± 2 due to the reduction in face area, resulting in an increase of the refractive index from 1.8 ± 0.2 to 4.1 ± 0.1 . However, the scope for further increase in the permittivity is substantial, thus leading to opportunities for design control over a wide range of values of the permittivity, permeability, and refractive index. Hence, this provides a basis for the development of broadband metamaterials with bespoke electromagnetic

parameters for applications in the field of microwave transformation optics.

The authors wish to acknowledge the financial support of the EPSRC and DSTL for funding L.P.'s PhD studentship through the University of Exeter Doctorial Training account, and J.R.S., I.J.Y., and A.P.H. acknowledge the support by EPSRC through the QUEST Programme Grant (EP/I034548/1) "The Quest for Ultimate Electromagnetics using Spatial Transformations."

¹D. R. Smith, W. J. Padilla, D. C. Vier, S. C. N. Nasser, and S. Schultz, *Phys. Rev. Lett.* **84**, 4184 (2000).

²J. B. Pendry, A. Holden, D. Robbins, and W. Stewart, *IEEE Trans. Microwave Theory Tech.* **47**, 2075 (1999).

³V. G. Veselago, *Sov. Phys. Usp.* **10**, 509 (1968).

⁴A. Demetriadou and J. B. Pendry, *J. Phys.: Condens. Matter* **20**, 295222 (2008).

⁵M. Choi, S. H. Lee, Y. Kim, S. B. Kang, J. Shin, M. H. Kwak, K. Y. Kang, Y. H. Lee, N. Park, and B. Min, *Nat. Sci.* **470**, 369 (2011).

⁶A. Thaker, A. Chevalier, J. L. Mattei, and P. Queffelec, *J. Appl. Phys.* **108**, 014301 (2010).

⁷H. Chen, C. T. Chan, and P. Sheng, *Nat. Mater.* **9**, 387 (2010).

⁸J. B. Pendry and B. Wood, *J. Phys.: Condens. Matter* **19**, 076208 (2007).

⁹M. Lapine, A. Krylova, P. A. Belov, C. G. Poulton, R. C. Mc Phedran, and Y. S. Kivshar, *Phys. Rev. B* **87**, 024408 (2013).

¹⁰P. A. Belov, A. B. Slobozhanyuk, D. S. Filonov, I. V. Yagupov, P. V. Kapitanova, C. R. Simovski, M. Lapine, and Y. S. Kivshar, *Appl. Phys. Lett.* **103**, 211903 (2013).

¹¹J. Shin, J. Shen, and S. Fan, *Phys. Rev. Lett.* **102**, 093903 (2009).

¹²T. Cambell, A. P. Hibbins, J. R. Sambles, and I. R. Hooper, *Appl. Phys. Lett.* **102**, 091108(1) (2013).

¹³W. Barry, *IEEE Trans. Microwave Theory Tech.* **34**, 80 (1986).

¹⁴MATLAB R2012a, The MathWorks Inc. Natick, MA, 2012.

¹⁵ANSYS HFSS V14, Ansys Inc., Canonsburg, PA, 2011.